Use of gas sensors and FOBT for the early detection of colorectal cancer

G. Zonta[1,3]*, G. Anania[1], C. Feo[6], A. Gaiardo[1,3,5], S. Gherardi[3], A. Giberti[4], V. Guidi[1], N. Landini[1,3], C. Palmonari[1,2], L. Ricci, A. de Togni[2] and C. Malagù[1,3]

[1] *University of Ferrara, Via Savonarola 9 - 44121 Ferrara, Italy*
[2] *Department of Public Health (AUSL) - UO Igiene Pubblica - Via Fausto Beretta, 7 – 44121 Ferrara, Italy*
[3] *SCENT S.r.l., Via Quadrifoglio 11 – 44124 Ferrara, Italy*
[4] *MIST E-R s.c.r.l., Via P. Gobetti 101, 40129 Bologna, Italy*
[5] *MNF - Micro Nano Facility, Bruno Kessler Foundation, Via Sommarive 18, 38123 Trento, Italy*
[6] *Ospedale del Delta, Via Valle Oppio, 2 - Lagosanto FE, Italy*

Abstract

Among the major challenges of medicine today there is the early detection of tumors, in order to prevent their degeneration into malignant stages and/or metastases. In particular, the colorectal cancer shows a high curability rate, up to 90%, if identified when in stage I. This is the reason why a reliable screening protocol is strictly necessary to avoid colorectal cancer progression. The Protocol discussed here is proposed to implement the clinical validation of a device, consisting of an array of chemoresistive semiconductor gas sensors, capable of identifying the difference between fecal exhalation of healthy subjects and of subjects suffering from high-risk colorectal adenomas or cancers. The analysis done are compared to the results of fecal occult blood test and colonoscopy as a gold standard. The difference among the two classes of fecal samples is due to the presence of tumor gaseous biomarkers, produced by cancerous cells through membrane peroxidation process and metabolic alterations. Our method combines a specific algorithm appositely created for data acquisition with principal component analysis and support vector machine. The test resulted capable of recognizing all the colorectal cancer plus high risk adenomas and the 98% of healthy subjects. The recognition capability of low-risk adenomas is progressively increasing (45%) along with statistics.

Keywords: gas sensors; nanostructures; colorectal cancer; screening; FOBT; clinical validation

Presented at the Eurosensors 2017 Conference, Paris, France, September 3–6, 2017.

* Corresponding author. Tel. +39 0532 974286
Email address: giulia.zonta@unife.it

1. Introduction

The aim of a medical screening is to prevent tumor degeneration into incurable stages. According to American Cancer Society data, colorectal cancer (CRC) has been classified as the third most commonly diagnosed cancer type in USA. Moreover, the lifetime risk of developing CRC is of about 1 in 21 (4.7%) for men and 1 in 23 (4.4%) for women. On the other hand, if promptly diagnosed, CRC is also one of the most curable types of cancer (about 90% at stage I) and prevention is fundamental to avoid its degeneration [1]. About this, over the last decades, the search for cancer diagnosis by the detection of gaseous cancer biomarkers is extremely active. These biomarkers are volatile organic compounds (VOCs) produced by cancerous cells due to two main processes: i) membrane peroxidation; ii) metabolic alterations, and they can be found in human body fluids (e.g., breath, blood, urine, intestinal gases and feces) [2-12]. With the aim of identifying biomarkers presence in the body, nanostructured gas sensors could be the ideal candidates for the implementation of a diagnostic device, due to their sensitivity, versatility and the fast response outcome. Studies on the physics of nanostructures, both from the experimental and theoretical point of view, show the capability of semiconductor nano-powders to detect gases in lower concentration with respect to their coarser counterparts. This is due to surface effects, which can be explained with a treatment that is borderline between classic and quantum solid state physics. A brief theoretical explanation of their behavior is addressed in the present work.

The purpose of the present study is to discriminate healthy subjects from subjects affected by CRC since the stage of advanced adenoma, by means of a non-invasive method. Currently, the test accepted in Italy and other countries (e.g., UK, France) is the fecal occult blood test (FOBT). In Italy it is performed every two years on people between 50 and 69 years of age. In particular, in Ferrara (Italy), the immunochemical version of this screening (iFOBT or FIT) is active since 2004. This test uses antibodies to detect human hemoglobin protein in stool. Despite being a valid tool for detecting blood presence in the stool, FOBT shows a huge number of false positives [13, 14]. Therefore, the

importance of an additional screening system lies in the decrease of false positive rate, to reduce the number of non-operative colonoscopies, risky for elderly and debilitated patients. Previous works by our team have shown that chemoresistive sensors are capable of detecting tumor biomarkers in very low concentrations (up to tenths of ppb) [15, 16]. The technique presented here employs a patented device [17] named SCENT A1, made of a core of five chemoresistive sensors. SCENT A1 can identify cancer by the odor of fecal exhalations. The difference between fecal samples of healthy subjects and of CRC-affected patients is due to the mixture of VOCs produced by tumor cells. Here are shown both the data coming from a feasibility study to set-up the sensor array [18, 19] and the data obtained by a clinical validation Protocol, started in May 2015 and still on-going [20].

2. Materials and methods

The device SCENT A1 is equipped with a pneumatic system that allows sending an environmental airflow, contaminated by fecal fumes, to the sensing unit. It allows the casing of sensors combined in a 5-units array, whose negative interaction with external environment are reduced thanks to carbon filters and anti-bacterial filters of 0.2μm. Filtered air, inflated by a dedicated pump, flows through the circuit and transports the fecal exhalations from the box to the sensors chamber. Sensors vary their resistance in contact with the gas and can distinguish different mixtures. Each sensor is composed of a thick-film of nanostructured semiconductor material of printed onto an alumina substrate (sized 2,54 mm × 2,54 mm), two comb-shaped gold electrodes and a platinum heater to reach the desired operating temperature. In Figure 1 a schematic representation of the sensor on a top (a) and a bottom (b) view. Stool samples to be analyzed are conserved inside standard containers (ARTSANA SpA Feces Container STER 18140) and they must be immediately put inside a freezer, in order to inhibit bacterial activity. Half an hour before the beginning of analysis, feces can be defrosted and prepared inside the sample box of SCENT A1. The response (R) is calculated, for n-type sensors, as $\frac{\Delta G}{G}$, where

ΔG is the difference between conductance with VOCs-contaminated air (G_{gas}) and the conductance in environmental air (G). For *p*-types, R is the negative reciprocal of the previous quantity.

2.1. Feasibility study

Preparation and characterization of nanostructured sensors have been described in detail on other publications [21-29]. The feasibility study has been performed in order to find the best five-sensor combination, in collaboration with the Department of Morphology, Surgery and Experimental Medicine of the University of Ferrara (UNIFE). The first data analysis method chosen is the principal component analysis (PCA), through which it is possible to represent each sample tested as a point in a lower dimensional space of features and to identify two different ellipsoidal regions for healthy and CRC-affected individuals [30]. The smaller the overlap between the two areas and the greater the precision of the test. The chosen combination of sensors has been calibrated, after testing 19 different materials (both metal-oxides and -sulfides), so as to maximize the difference between the two sample types (feces of healthy subjects and subjects with CRC, taken during surgery), thanks to an activity previously carried out in the laboratory on 170 samples [18, 19]. The PCA related to one of the most discriminating arrays is shown in Figure 2. The parameter chosen for PCA analysis are the response values of the sensors in the chosen array. The green dots represent 18 control samples while the blue ones are 10 samples from subjects with CRC. The areas identify the two populations and the overlap is minimal. This is indicative of a high degree of distinction. The ROC curve, in Figure 3, was calculated by considering all the sample tested with all the sensor arrays tried. The curve shows both a sensitivity and a specificity of 95% and also the accuracy of the test has been estimated as 95%. The materials chosen after this study were both single metal-oxides and mixtures of them (i.e., indium, tin, titanium and vanadium oxide), fired at a temperature of 650 °C (see Table 1). SEM images of these materials are shown in Figures 4-8. All materials show a nanostructured geometry, in order to increase the available surface on which chemical reactions between the material and the gas occur. In particular, all the material are composed of nanograins, except for In_2O whose structure

is composed by fibers with a nanometric section. In Figure 9 an example of the voltage curve trends for SCENT A1 sensors, before response elaboration. It is noticeable that only one of the sensors show a p-type behavior.

2.2. Clinical validation

After this first step an algorithm for data acquisition has been developed in LabVIEW. This software, is able to real time calculate and register different features for each sensor, based on their electrical signals (response at 90%, derivative, integral and time at which these parameters have been taken). A total of twenty features is then processed with support vector machine (SVM) algorithm, in order to maximize the geometric margin while minimizing the empirical classification error [31]. In Figure 10 an example of these parameters for a single sensor (ST20) after a test with the device. Since May 2016, following the approval by the Ethics Committee, it has been started a Protocol for the clinical validation of the device. To all of screening users in Ferrara, who resulted positive to FOBT, is proposed to participate in the experimental study SCENT A1 before undergoing colonoscopy investigation (chosen as the gold standard). Over 90% of patients have adhered to the study. Colonoscopy results are fundamental to obtain a sufficient statistic to calibrate the device and to set a priori the accuracy of the method. In addition to SCENT A1 tests, a volunteer physician, engaged in the interview with the patients, developed an assessment based on questions submitted to the subjects. These questions concern familiarity, symptoms and other inflammatory diseases suffered from patients. A comparison between evaluations obtained through this medical consultation and colonoscopy outcomes may provide added value to the fundamental importance of a screening test. The sensitivity and specificity of an expert eye are respectively of 11 and 96%, evaluated on a sample of 131 subjects, of which we had both the doctor's overthrow and the colonoscopy outcome. If only the average/high risk adenomas and cancers are considered as positives, the sensitivity results null.

This qualitative data gives an idea of the crucial importance of a preventive screening for CRC to avoid a so large number false negatives. So far, the sensor responses of a total of 238 fecal samples have been measured with SCENT A1 during the Protocol. The precision of FOBT test estimated from the data that have already a colonoscopy result (174) is only of 28%. This means that the number of false positives is very high and this involves a large number of non-operative colonoscopies, submitting healthy patients to an unnecessary risk of intestinal perforation. The addition of a complementary test, i.e. SCENT A1, relying on a gaseous marker totally different from occult blood, should be fundamental to reduce false positive rate.

2.3. Theoretical approach

The sensors selected for SCENT A1 arrays are all of metal-oxide type, even if in the feasibility study also metal-sulfide semiconductor have been tested [18]. In the sensing mechanisms of metal-oxide nanopowders it is fundamental to take on account mechanisms of in- and out-diffusion, due to the presence of oxygen vacancies. This phenomenon is crucial to estimation the correct response value in a reliable way. Some tests with *n-type* semiconductors have shown that there are two different types of different trends in resistance when placed in synthetic dry air (23% O_2 and 77% N_2) after exposition to inert atmosphere (99% N_2 and 1% O_2) [32, 33]. Starting from the equilibrium equation of the process and working out the mass action law, $K = [V^{++}]n^2p(O_2)^{1/2}$, it is apparent that, as the mobile charge density (n) goes to zero due to the action of the built-in field, the density of oxygen vacancies $[V^{++}]$increases strongly at constant oxygen partial pressure, $p(O_2)$. This results in a non-uniform vacancy profile inside a grain which increases from the bulk towards the surface that can be extrapolated by placing it into the Poisson Equation. The ionized donor concentration has the shape: $c(x) = N_d \exp(2\mathrm{eV}(x)/\mathrm{kT})$, where N_d is the density of oxygen vacancies in the bulk and $V(x)$ the built-in potential in the space charge region at a distance x from the edge of the bulk. After dividing the band bending by the electron charge (e) the surface potential (V_S) results: $V_S = \frac{\mathrm{kT}}{2e}\ln[1 + \frac{N_t}{8N_d^2 L_D{}^2})]$, being L_D the Debye length for *n*-type majority carriers and N_t the density of surface states. The Fermi level

position, E_F, with respect to the conduction band minimum in the bulk, E_{CB}, can be derived by considering neutrality condition. Finally, by considering that all donors are ionized at working temperature (ranging from 350 to 450°C for SCENT A1 sensors), the total Schottky barrier height, $S_B = V_S + E_{\mathrm{CB}} - E_F$ can be found.

The trend of S_B versus the relative oxygen pressure before and after in-diffusion (equilibrium) are two straight lines completely different from each other, in fact before diffusion the slope is smaller. This leads to an explanation of the two different trends in resistance for *n*-type semiconductors changing from dry air to inert atmosphere. The first it is an upwards drift of the resistance that that take place after oxygen chemisorption due to in-diffusion allowed by high working temperature. The second phenomenon takes place if the grains are sufficiently large that the depletion region width, Λ, is initially smaller than the grain radius, *R*. In diffusion leads to the condition Λ=*R* and at this point a novel phenomenon may be responsible for a decrease in resistance observed after injecting oxygen. This is due to an asymmetrical voltage drop as soon as a grain is sufficiently large (not to be fully depleted), described in detail in Ref. [32, 33]. The result is that when a grain becomes completely depleted by means of in-diffusion process this asymmetry is expected to disappear. This leads to a decrease in resistance due to the increase of one of the two terms inside current equation [32, 33]. This model allowed us to determine the critical average grain size of a material in order to avoid the main source of instability of the signal. This helped us perform medical measurements with a reliable methodology.

3. Experimental results and discussion

Since now, 86 of the samples measured with SCENT A1 have been compared with the gold standard. They have been analyzed by means of PCA and Support Vector Machine (SVM) techniques, dividing the three class of subjects:

- cancer and high-risk adenomas (CRC+HR);

- low-risk adenomas (LR);
- healthy subjects (HS).

In this first step SVM is employed an indicator of how well data is classified, labeling a priori their health status as indicated by colonoscopy. Results are summarized in the confusion matrix in Figure 11. The confusion matrix plots the "actual class", so the colonoscopy outcomes, versus the "predicted class", resulted by the tested algorithm. In the diagonal of the matrix are shown the correct predictions. It appears evident from these data, that all the CRC+HR are correctly identified so as the largest part of HS (98%). Only LR show here only a percentage of 10%. The error on LR is not so problematic, in fact, for low risk adenomas, the risk for degeneration is negligible. For this reason, classifying subjects with low risk adenomas as healthy and re-screening them after two years, it could be a way of reducing colonoscopies to the benefit of the patients' health. This data set will serve as a basis for predicting the health status of subjects before knowing the colonoscopy outcome.

From September 2017, the Protocol has been extended to Ospedale del Delta in Lagosanto (Italy), with the aim of increasing the statistics on true positives. Since now, two fecal samples of CRC-affected subjects have been tested. In order to validate the statistics obtained through SVM, the new samples were inserted into the training method without any label. The results were encouraging, as the algorithm recognized both of them as positives. In Table 2 are shown the classification probabilities for the two samples. Moreover, by inserting these two new data into the previous statistic, it has been obtained a new forecast basis for future sample classification (Figure 12). Now the recognition capability of LR is of 45%, as the addition of new data allows to increase the degree of system information, improving its accuracy.

The clinical validation will continue for two years. In Table 3, it is reported a comparison of the data obtained so far from the present study. These data will be progressively updated during the continuation of the tests. In the future, the protocol will also be extended to the FOBT negative analysis.

4. Conclusions

This work represents a deepening of a medical application of chemoresistive gas sensor technology. The device SCENT A1, composed by a core of semiconductor nanostructured gas sensors, has been tested for the early-screening of CRC through the odor of fecal samples. After being subjected to a feasibility study with samples taken during surgery for selecting the most discriminating sensor array, the device is now undergoing clinical validation. The protocol consists in the analysis of stool samples exhalations from subjects resulted positives to FOBT and the subsequent comparison of the results with colonoscopy as a gold standard. The protocol is started in May 2016 and it is still ongoing with an extension to Ospedale del Delta in September 2017 in order to raise the statistics on true positives. The main results onto 88 tests, obtained through the combination of a specific algorithm for data collection realized by our group with the SVM technique, is highly encouraging. Even if the recognition capability for low risk adenomas (45%) should be improved by increasing the global statistics, the device was able to recognise all CRC and high risk adenomas and the 98% of healthy subjects that was judged positives by FOBT. This fact demonstrates that the combination of the in-vitro analysis SCENT A1 with FOBT could lead to a reduction of more than 65% of non-operative colonscopies, performed in-vivo on healthy patients. Moreover, a parallel in interview to patients who adhere to the Protocol, made by a volunteer physician before colonoscopy, show that even an expert eye cannot identify a CRC only analysing symptoms and familiarity (only 11% of sensitivity), underlying the fundamental importance of a reliable screening method.

In the next future, further researches will be aimed at determining the surface reactions responsible for the different trend of sensor responses with diverse fecal samples. In particular, thanks to the different composition of sensor marterials, phenomena of catalysis that might occur between the surface and the heathen environment will be explored. After these considerations, the study of reactions with the use of FTIR (Fourier Transform Infrared Spectroscopy) appears as a viable option, together with Gas Chromatographic (GC) analysis to state the differences of gas concentration in the

circuit lines and in the sensors chamber.

5. References

[1] http://www.cancer.org/cancer/colonandrectumcancer/detailedguide/colorectal-cancer-key-statistics;

[2] T. G. de Meij, I. Ben Larbi, M. P. van der Schee, Y. E. Lentferink, T. Paff, J. S. Terhaar sive Droste, C. J. Mulder, A. A. van Bodegraven and N. K. de Boer, Electronic nose can discriminate colorectal carcinoma and advanced adenomas by fecal volatile biomarker analysis: proof of principle study, International Journal of Cancer (2014), 134, 1132–1138;

[3] G. Peng and M. Hakim, Detection of lung, breast, colorectal, and prostate cancers from exhaled breath using a single array of nanosensors, British Journal of Cancer, 103 (2010) 542-551;

[4] D. F. Altomare and M. Di Lena, Exhaled volatile organic compounds identify patients with colorectal cancer, Wiley Online Library (2013);

[5] G. Tonini, F. Siqueira, Evaluation of computer methods for biomarker discovery on computational grids, Electronic Journal of Biotechnology (2013), ISSN: 0717-3458, Vol. 16 No. 5;

[6] H. Haick, Y. Y. Broza, P. Mochalsky, V. Ruzsanyi and A. Amann, Assessment, origin and implementation of breath volatile cancer markers, Chemical Society Reviews (2014), 43, 1423-1449;

[7] B. Tan, Y. Qiu, X. Zou, T. Chen, G. Xie, Y. Cheng, T. Dong, L. Zhao, B. Feng, X. Hu, L. X. Xu, A. Zhao, M. Zhang, G. Cai, S. Cai, Z. Zhou, M. Zheng, Y. Zhang, W. Jia, Metabonomics identifies serum metabolite markers of colorectal cancer, J Proteome Res. (2013), 12(6):3000-9;

[8] B. Szachowicz-Petelska, I. Dobrzyńska, S. Sulkowski, Z. A. Figaszewski, Characterization of the Cell Membrane During Cancer Transformation, NMR in Biomedicine V5, Issue 5, 226–233, September/October 1992;

[9] B. Tan, Y. Qi, X. Zou, T. Chen, G. Xie, Y. Cheng, T. Dong, L. Zhao, B. Feng, X. Hu, L.X. Xu, A. Zhao, M. Zhang, G. Cai, S. Cai, Z. Zhou, M. Zheng, Y. Zhang, W. Jia, Metabonomics identifies serum metabolite markers of colorectal cancer, Journal of Proteome Research (2013), 12(6), 3000-9;

[10] C. SJ. Probert, I. Ahmed, T. Khalid, E. Johnson, S. Smith, N. Ratcliffe, Volatile Organic

Compounds as Diagnostic Biomarkers in Gastrointestinal and Liver Diseases (2009), 18(3), 337-43;

[11] A.B. Sahakian, S. R. Jee, M. Pimentel, Methane and the Gastrointestinal Tract, Digestive Diseases and Sciences (2010), 55(8), 2135-43;

[12] J. Vermeiren, T. Van deWiele, W. Verstraete, P. Boeckx, N. Boon, Nitric Oxide Production by the Human Intestinal Microbiota by Dissimilatory Nitrate Reduction to Ammonium, Journal of Biomedicine and Biotechnology Volume 2009 (2009);

[13] S. H. Elsafi, N. I. Alqahtani, N. Y. Zakary and E. M. Al Zahrani, The sensitivity, specificity, predictive values, and likelihood ratios of fecal occult blood test for the detection of colorectal cancer in hospital settings, Clin Exp Gastroenterol., 8: 279–284, 2015;

[14] A. Shin, K. Son Choi, J. Kwan Jun, D. Keun Noh, M. Suh, K.W. Jung, B. Chang Kim, J. Hwan Oh, E. C. Park, Validity of Fecal Occult Blood Test in the National Cancer Screening Program, Korea, PLoS One, 8(11): e79292, 2013;

[15] C. Malagù, B. Fabbri, S. Gherardi, A. Giberti, V. Guidi, N. Landini, G. Zonta, Chemoresistive gas sensors for detection of colorectal cancer biomarkers, Sensors, 14, 18982-18992, 2014;

[16] G. Zonta, G. Anania, B. Fabbri, A. Gaiardo, S. Gherardi, A. Giberti, V. Guidi, N. Landini, C. Malagù, Detection of colorectal cancer biomarkers in the presence of interfering gases, Sensors and Actuators B, 218, 289-295, 2015;

[17] SCENT A1, patent number: RM20144000595, patent and intellectual property of SCENT S.r.l., European internationalization in progress;

[18] N. Landini, G. Zonta, C. Malagù (2015), Detection of tumor markers on feces with nanostructured sensors, Scholars' Press, ISBN-13: 978-3-639-76538-0;

[19] G. Zonta, G. Anania, B. Fabbri, A. Gaiardo, S. Gherardi, A. Giberti, N. Landini, C. Malagù, L. Scagliarini, V. Guidi, Preventive screening of colorectal cancer with a device based on chemoresistive sensors Sensors and Actuators B, 238, 1098–110, 2016;

[20] Acceptance Letter from the Ethics Committee of Ferrara (2016), "Valutazione dell'accuratezza della determinazione di composti organici volatili quali biomarker di neoplasia colo-rettale nelle feci di soggetti FOBT-positivi sottoposti a colonscopia";

[21] G. Ghiotti, A. Chiorino, Preparation and characterization of WOx/SnO2 nanosized powders for thick films gas sensor, Studies in Surface Science and Catalysis (2001), 140, 287–296;

[22] M. Benetti, M. Blo, Symplectic gel co-precipitation of TixSn1−xO2 solid solutions for gas sensing. In Proceedings of the Eurosensors XIX, Barcelona, Spain, 11–14 September (2005);

[23] M. C. Carotta, M. Benetti, Nanostructured (Sn, Ti, Nb)O2 solid solutions for hydrogen sensing. In Proceedings of the Materials Research Society Spring Meeting, S. Francisco, CA, USA, 17–21 April (2006), p. 68210;

[24] M. C. Carotta, A. Cervia, V. di Natale, S. Gherardi, A. Giberti, V. Guidi, D. Puzzovio, B. Vendemiati, G. Martinelli, M. Sacerdoti, D. Calestani, A. Zappettini, M. Zha, L. Zanotti, ZnO gas sensors: A comparison between nanoparticles and nanotetrapods-based thick films, Sensors and Actuators B (2009), 137, Issue 1, pp 164–169;

[25] M. C. Carotta, M. Feroni, D. Gnani, V. Guidi, M. Merli, G. Martinelli, M. C. Casale, M. Notaro, Nanostructured pure and Nb-doped TiO2 as thick film gas sensors for environmental monitoring, Sensors and Actuators B (1999), 58, 310-317;

[26] M. C. Carotta, V. Guidi, Vanadium and tantalum-doped titanium oxide (TiTaV): A novel material for gas sensing. Sensors and Actuators B (2005), 108, 89–96;

[27] V. Guidi, C. Malagu', M.C. Carotta, B. Vendemiati, Printed films: Materials science and applications in sensors, electronics and photonics, in Woodhead publishing series in electronic and optical materials (2012), pp.278-334;

[28] M. C. Carotta, A. Cervi, Metal-oxide solid solutions for light alkane sensing. Sensors and Actuators B (2008), 133, 516–520;

[29] M.C. Carotta, A. Cervi, Ethanol interference in light alkane sensing by metal-oxide solid solutions. Sensors and Actuators B (2009), 136, 405–409;

[30] A. J. Izenman, Modern Multivariate Statistical Techniques, Springer-Verlag New York (2008), ISSN 1431-875X, ISBN 978-0-387-78188-4, DOI 10.1007.978-0-387-78189-1;

[31] B. Scholkopf, A. J. Smola, Learning With Kernels: Support Vector Machines, Regularization, Optimization and Beyond (2001), ISBN: 9780262253437;

[32] C. M. Aldao and C. Malagù, Non-parabolic intergranular barriers in tin oxide and gas sensing, Journal of Applied Physics, 112, 2012, p. 024518;

[33] C. Malagù, A. Gaiardo, S. Gherardi, A. Giberti, N. Landini, C. Palmonari, G. Zonta, Mechanisms of response of chemoresistive gas sensors applied to colorectal cancer screening, 3rd International Conference on Sensors Engineering and Electronics Instrumentation Advances (SEIA' 2017), 20-22 September 2017, Moscow, Russia

6. Figure captions

Fig. 1: Schematic representation of the sensor on a top (a) and a bottom (b) view.

Fig. 2: PCA related to the chosen array. Here are shown 18 control samples (green dots) and 10 samples from subjects with CCR (blue dots). The areas represent the two populations. The overlap between the two classis is minimal.

Fig. 3: Confusion matrix (on the left) and ROC curve (on the right) made with 157 samples with different five-sensor combinations of 19 materials. True Positive Rate (TPR) = sensitivity = 95%, True Negative Rate (TNR) = specificity = 95%.

Fig. 4: SEM images of SmFeO3 sensor powder. It is noticeable the granular nanometric structure with high degree of homogeneity.

Fig. 5: SEM images of TiTaV sensor powder. The combination of diverse oxides in this solid solution confer to the material a non-homogeneous macroscopic geometry, composed of an internal structure of nanograins.

Fig. 6: SEM images of ST20 sensor powder. The structure is composed by spherical agglomerations of different dimensions. Each one is composed of an internal structure of homogeneous nanograins.

Fig. 7: SEM images of In_2O powder. The geometry of this oxide is composed of cubes and parallelepipeds. The structures of these macro-geometries are composed by fibers with nanometric sections.

Fig. 8: SEM images of ST25+Au sensor powder. The structure of this material is highly homogeneous and each particle agglomeration is composed by nanograins.

Fig. 9. Example of the voltage curve trends (V_{out}) with time for SCENT A1 sensors with a fecal sample, before response elaboration.

Fig. 10. Response at 90% (*R*), derivative (*D*) and integral (*I*) vs time at which the parameters have been taken (in seconds) for a single sensor (ST20) measured during a test of the clinical validation protocol.

Fig. 11. Confusion matrix of the three classes of 86 fecal samples with the SVM method, where *LR* are low risk adenomas, *HS* are healthy subjects and *CRC+HR* are colorectal cancer and high risk adenomas. This classification has been performed by knowing a priori the colonoscopy response.

Fig. 12. Confusion matrix of the three classes of 88 fecal samples with the *SVM* method, where LR are low risk adenomas, *HS* are healthy subjects and *CRC+HR* are colorectal cancer and high risk adenomas. This classification has been performed by knowing a priori the colonoscopy response.

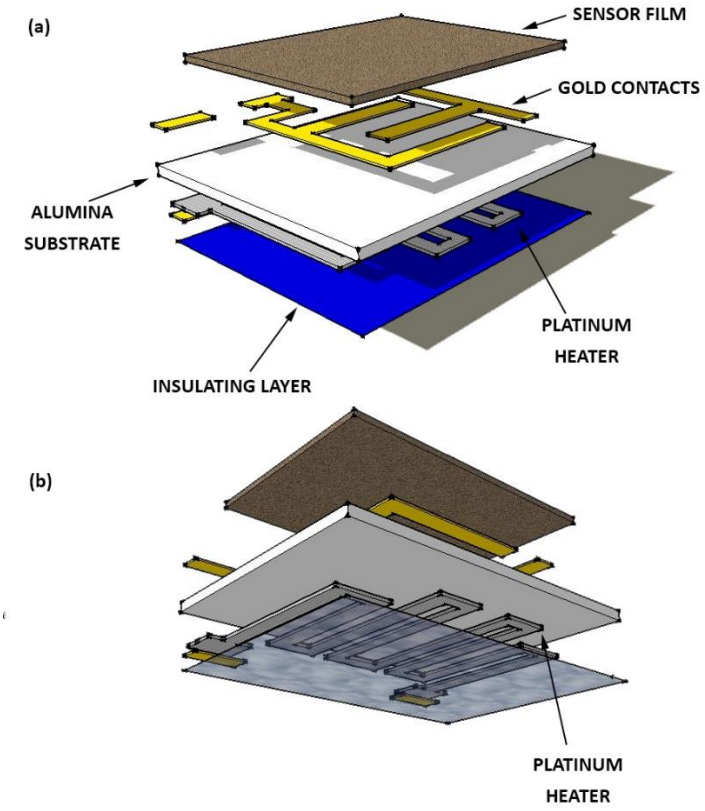

Figure 1

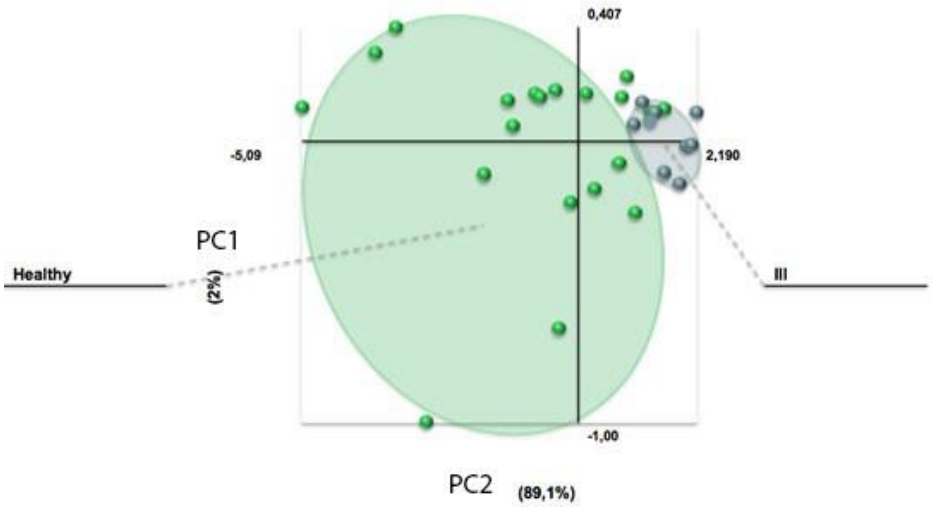

Figure 2

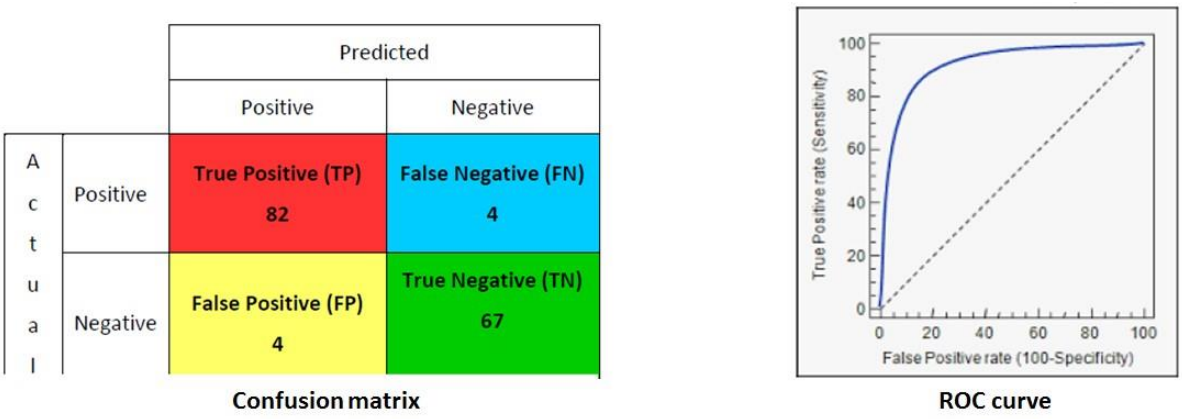

Figure 3

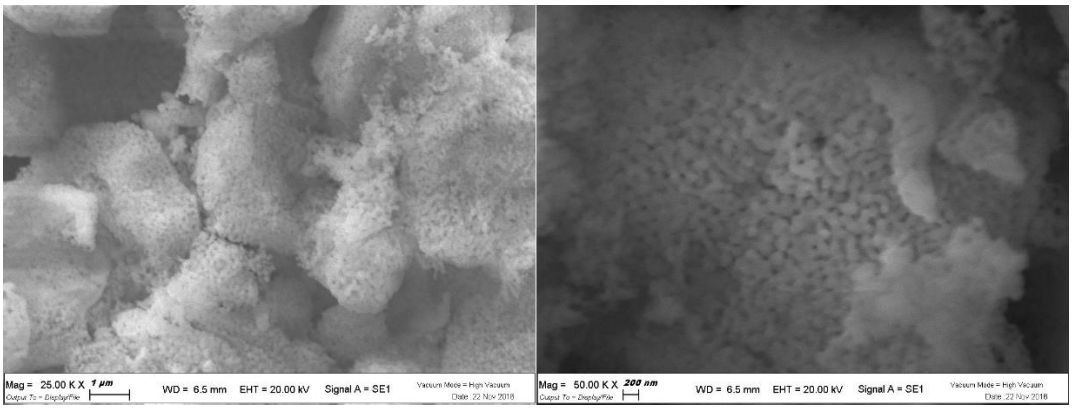

Figure 4

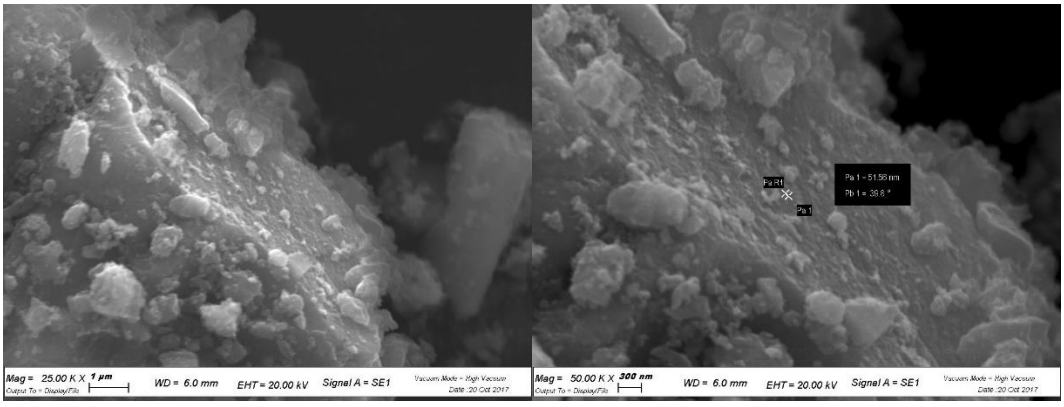

Figure 5

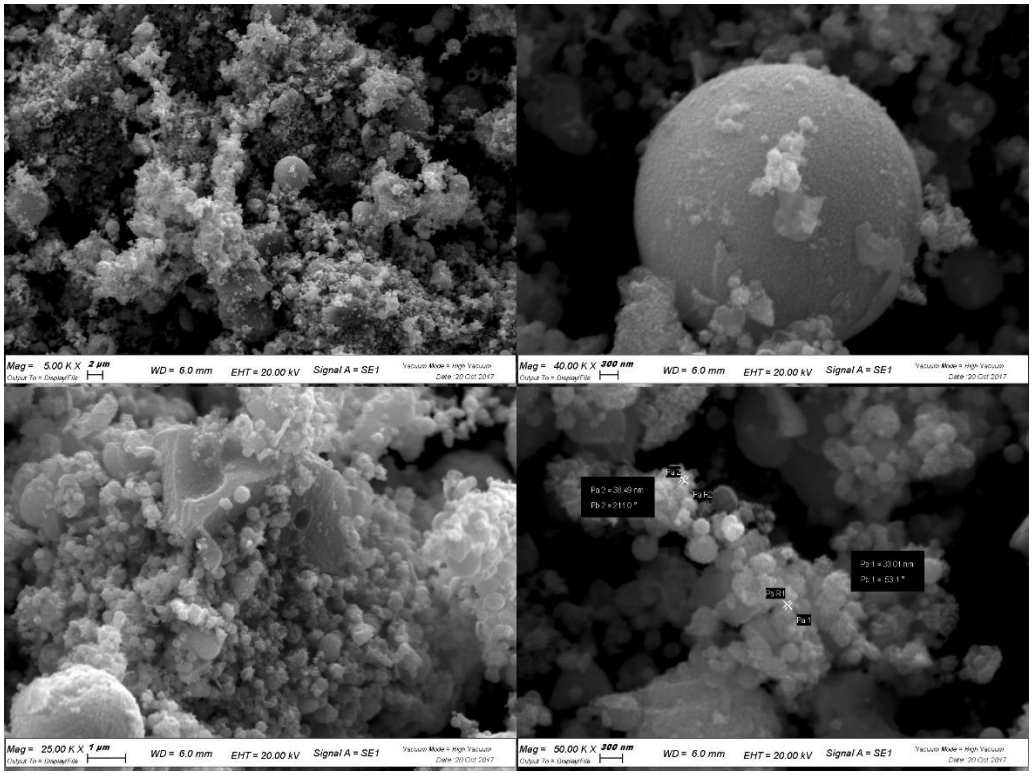

Figure 6

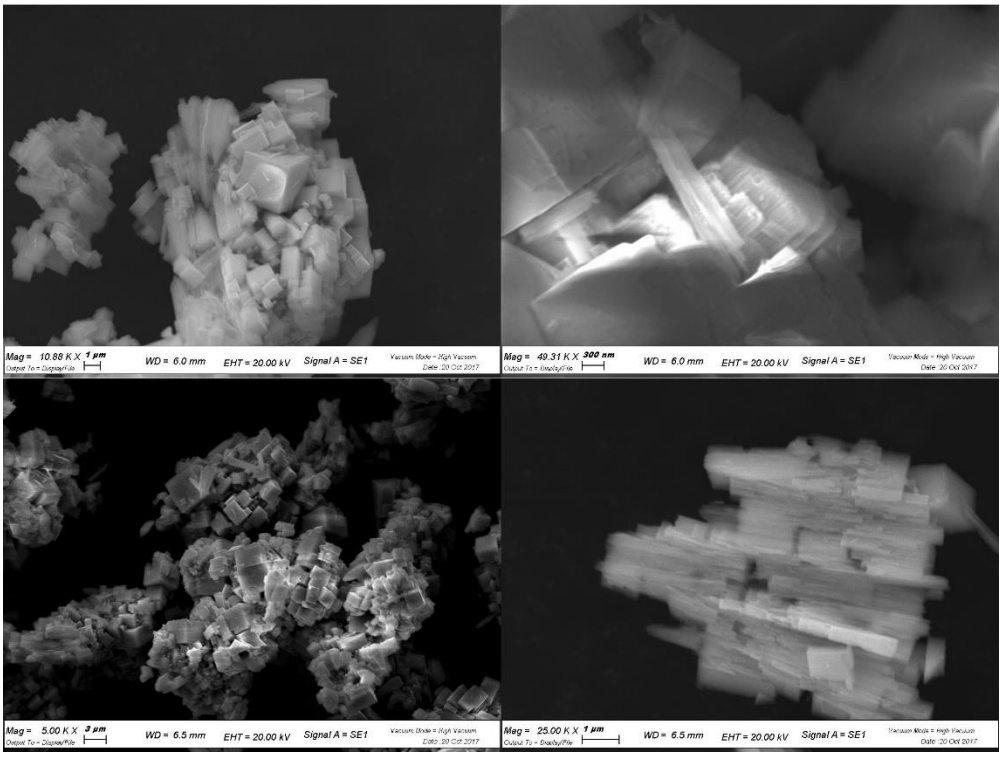

Figure 7

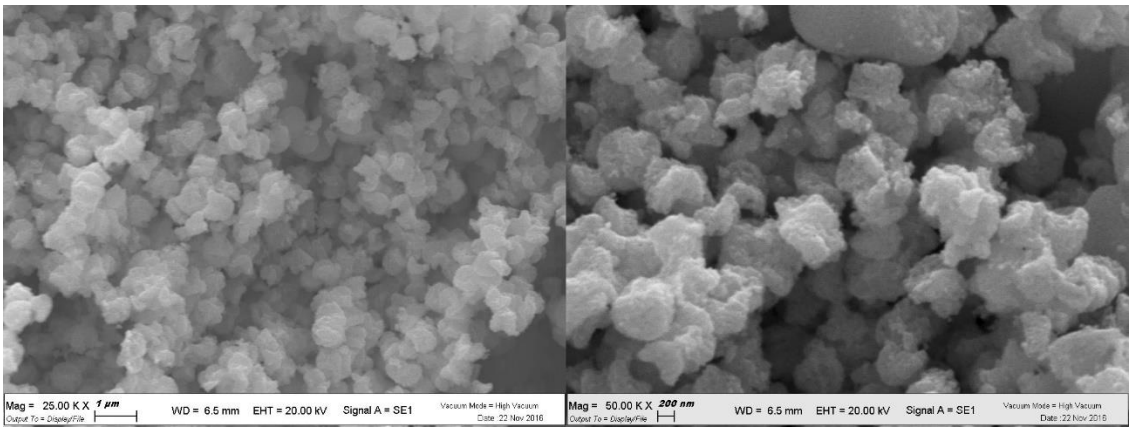

Figure 8

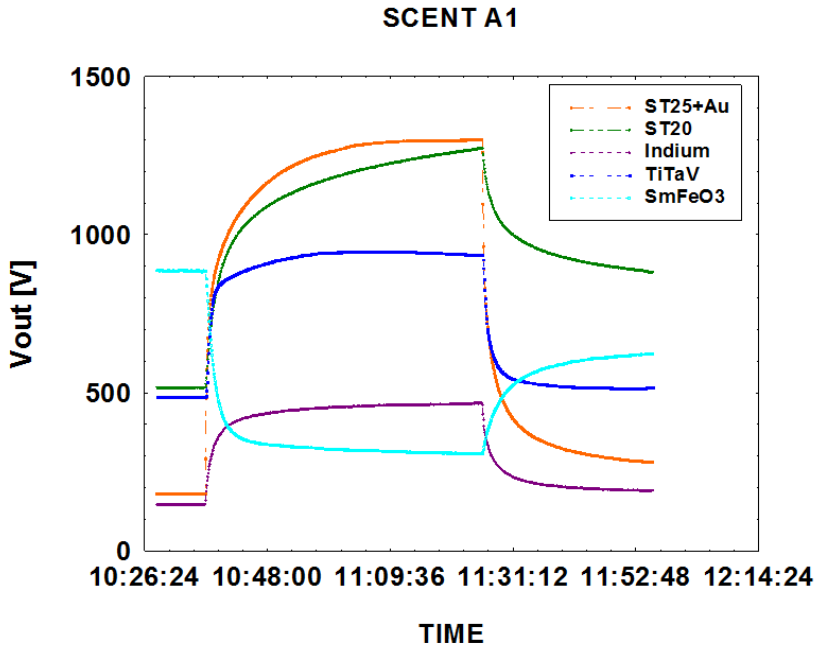

Figure 9

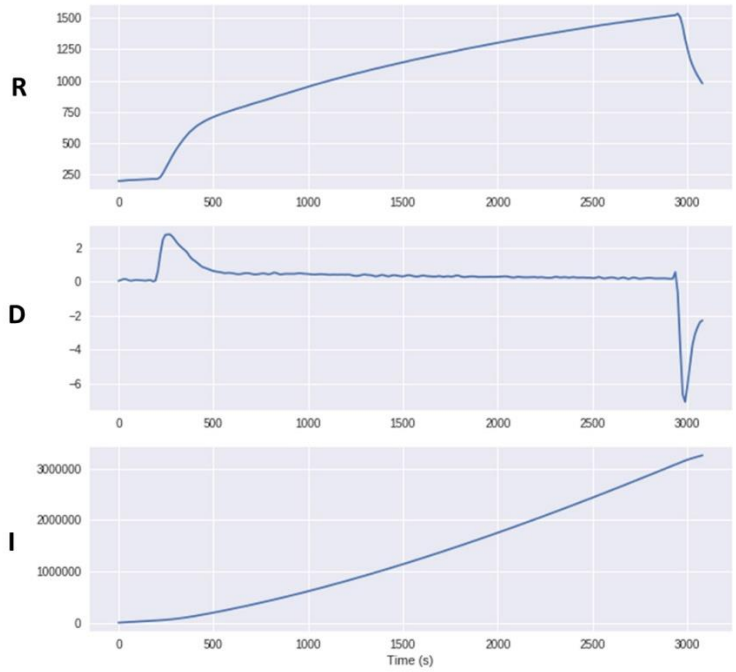

Figure 10

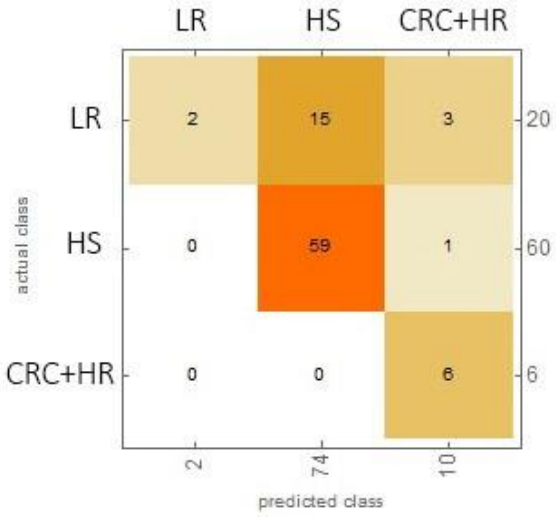

Figure 11

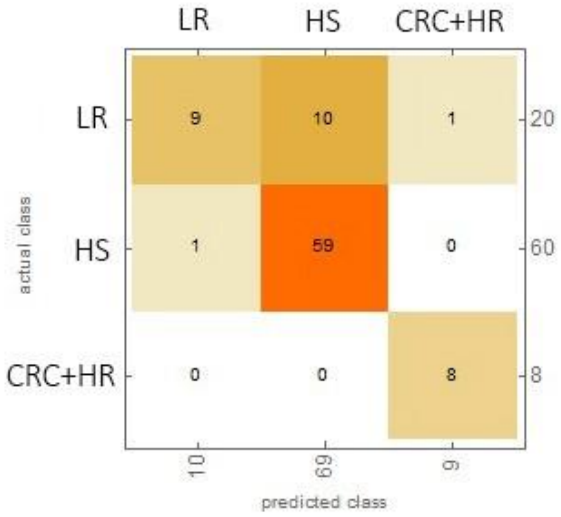
LR
HS
CRC+HR
LR
HS
CRC+HR
9
10
1
1
59
0
0
0
8
20
60
8
actual class
10
69
9
predicted class

Figure 12

Tables

Table 1. List of sensors chosen for the most performing array for SCENT A1 as a result of a feasibility study. These sensors are used in the clinical validation protocol tests.

CODE	WORKING T (°C)	MATERIALS	NANOSTRUCTURE AVERAGE SIZE (nm)
SmFeO3	350	Iron and Samarium oxides	63
TiTaV	450	Titanium, tantalum and vanadium oxides	52
ST20	450	Tin and Titanium oxide (20%)	36
In2O3	350	Indium Oxide	53
ST25 + Au	450	Tin and Titanium oxide (25%) with the addition of gold nanoparticles	30

Table 2. Classification probabilities of the two CRC-affected subject samples from Ospedale del Delta in Lagosanto.

	PROBABILITIES		
SAMPLE	**CRC+HR**	**LR**	**HS**
1	0.47	0.11	0.41
2	0.71	0.35	0.25

Table 3. Comparison of FOBT with the SCENT A1 data of feasibility study and patients' health evaluation during the interview. Samples are all from patients resulted positive to FOBT, so it is possible to estimate only the precision for this test. Data coming from the clinical validation of SCENT A1 are not shown due to the fact that they are split in three categories.

	FOBT	**SCENT A1**	**INTERVIEW**
Sensitivity (TPR)	-	95%	11%
Specificity (TNR)	-	95%	96%
Accuracy	-	95%	72%
Precision	28%	95%	44%